Oxygen Switching of the Epitaxial Graphene-Metal Interaction

ARTICLE *in* ACS NANO · OCTOBER 2012

Impact Factor: 12.88 · DOI: 10.1021/nn302729j · Source: PubMed

Oxygen Switching of the Epitaxial Graphene–Metal Interaction

Rosanna Larciprete,[†] Søren Ulstrup,[‡] Paolo Lacovig,[§] Matteo Dalmiglio,[§] Marco Bianchi,[‡] Federico Mazzola,[‡] Liv Hornekær,[‡] Fabrizio Orlando,[⊥,∥] Alessandro Baraldi,[⊥,∥] Philip Hofmann,[‡] and Silvano Lizzit[§,*]

[†]CNR-Institute for Complex Systems, Via Fosso del Cavaliere 100, 00133 Roma, Italy, [‡]Department of Physics and Astronomy, Interdisciplinary Nanoscience Center, Aarhus University, 8000 Aarhus C, Denmark, [§]Sincrotrone Trieste, S.S. 14 Km 163.5, 34149 Trieste, Italy, [⊥]Physics Department and Center of Excellence for Nanostructured Materials, University of Trieste, Via Valerio 2, 34127 Trieste, Italy, and [∥]IOM-CNR Laboratorio TASC, Area Science Park, S.S.14 Km 163.5, 34149 Trieste, Italy

ABSTRACT Using photoemission spectroscopy techniques, we show that oxygen intercalation is achieved on an extended layer of epitaxial graphene on Ir(111), which results in the "lifting" of the graphene layer and in its decoupling from the metal substrate. The oxygen adsorption below graphene proceeds as on clean Ir(111), giving only a slightly higher oxygen coverage. Upon lifting, the C 1s signal shows a downshift in binding energy, due to the charge transfer to graphene from the oxygen-covered metal surface. Moreover, the characteristic spectral signatures of the graphene–substrate interaction in the valence band are removed, and the spectrum of strongly hole-doped, quasi free-standing graphene with a single Dirac cone around the $\bar{K}$ point is observed. The oxygen can be deintercalated by annealing, and this process takes place at around $T = 600$ K, in a rather abrupt way. A small amount of carbon atoms is lost, implying that graphene has been etched. After deintercalation graphene restores its interaction with the Ir(111) substrate. Additional intercalation/deintercalation cycles readily occur at lower oxygen doses and temperatures, consistently with an increasingly defective lattice. Our findings demonstrate that oxygen intercalation is an efficient method for fully decoupling an extended layer of graphene from a metal substrate, such as Ir(111). They pave the way for the fundamental research on graphene, where extended, ordered layers of free-standing graphene are important and, due to the stability of the intercalated system in a wide temperature range, also for the advancement of next-generation graphene-based electronics.

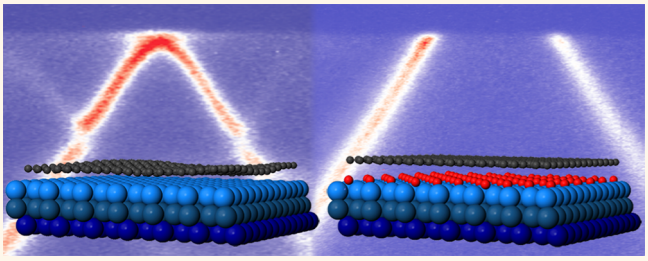

KEYWORDS: epitaxial graphene · Ir(111) · oxygen intercalation · doping · angle-resolved photoemission spectroscopy · X-ray photoelectron spectroscopy

The epitaxial growth of large-area, single-crystal graphene with excellent quality[1,2] is now routinely achieved on various transition metal surfaces[3−7] as well as on SiC.[8−11] Epitaxial graphene has certain advantages over exfoliated graphene on SiO_2,[12] especially when it comes to spectroscopic studies or device fabrication where the large area is important. Moreover, it is possible to tailor the graphene–surface interaction and the doping and to control the crystalline quality,[13] aspects that are important for the carrier mobility of supported graphene.[14,15]

Epitaxial graphene frequently exhibits a strong interaction with the substrate. In the most extreme cases, the interaction is sufficiently strong to prevent the characteristic electronic properties from being established, such as for a single graphene layer on SiC[9] or for epitaxial graphene on Ru(0001),[4] Rh(111),[16] and Re(0001).[17] For a weaker interaction, graphene-like electronic properties are observed, but the lattice incommensurability between graphene and its substrate gives rise to a moiré that changes the ideal linear band dispersion of the π-electrons in pristine graphene and gives rise to replica bands and minigaps near the Fermi level, as observed on Ir(111).[18,19] For some substrates, such as Pt(111),[20] the interaction with epitaxial graphene is very weak, thus leading to a lack of order and to the formation of graphene domains with different orientations. It is thus difficult to achieve a weak interaction with high structural quality at the same time.

A possible solution to this dilemma is the epitaxial growth of graphene on a metal substrate with a sufficiently strong interaction

* Address correspondence to lizzit@elettra.trieste.it.

Received for review June 20, 2012 and accepted October 10, 2012.

Published online October 10, 2012
10.1021/nn302729j

with graphene and the subsequent decoupling by the intercalation of metals[21−25] or silicon.[26] For graphene grown on SiC, it has been demonstrated that also atoms such as fluorine[27] or hydrogen[28] efficiently intercalate through the graphene layer. This has been shown to recover the pristine linear band dispersion, at least partly, and new phenomena could be observed only because of the quasi free-standing electronic structure achieved by the decoupling with hydrogen.[29]

Oxygen intercalation promises to play a similar role for graphene on transition metal surfaces, but so far intercalation has been shown only for incomplete monolayers or islands.[30−32] Here we demonstrate that intercalation is also possible for a complete graphene layer on Ir(111) at a certain temperature and for a sufficiently high oxygen partial pressure, leading to an intact but entirely free-standing layer with the corresponding electronic properties, *i.e.*, with the disappearance of the characteristic moiré-induced features in the electronic band structure. It is also possible to reverse the process by deintercalating and desorbing the oxygen. This process restores the original electronic properties of graphene on Ir(111), but it is accompanied by a moderate etching of the graphene lattice, making further intercalation processes possible at lower temperature and pressure.

RESULTS AND DISCUSSION

The oxygen intercalation on a complete monolayer of graphene/Ir(111) is studied by high-resolution X-ray photoelectron spectroscopy (XPS). As described in the Methods, the completeness of the layer was stated by XPS with an uncertainty of 1−2%. In order to establish the intercalation conditions, the C 1s, Ir $4f_{7/2}$, and O 1s core level spectra are measured for graphene exposed to molecular oxygen at different substrate temperatures. We find that the intercalation is possible only at a sufficiently high temperature. The results of different oxygen exposures are shown in Figure 1. The C 1s spectrum measured on the clean graphene shows a single, narrow peak at a binding energy (BE) of 284.14 eV (Figure 1a), whereas the corresponding Ir $4f_{7/2}$ spectrum exhibits components due to bulk (B) and first-layer Ir atoms (S) at 60.84 and 60.31 eV, respectively (Figure 1b).[33] The exposure through a doser to $\sim 5 \times 10^{-3}$ mbar of molecular oxygen at 430 K for 10 min causes merely the appearance of weak and broad features between 284.4 and 285.2 eV in the C 1s spectrum and between 530.5 and 533.0 eV in the O 1s spectrum (Figure 1c) due to the formation of C−O bonds in graphene/Ir(111).[34] The lack of any intensity at around 530 eV in the O 1s spectrum and of the surface core level shifted components related to adsorbed oxygen in the Ir $4f_{7/2}$ core level, which would indicate the dissociative adsorption of O atoms on Ir(111),[35] excludes the presence of bare substrate regions and further confirms the completeness of the graphene monolayer. After an equivalent exposure at 470 K, some O_2 molecules effectively penetrate below graphene and dissociatively chemisorb on the Ir surface, as witnessed by the O 1s peak at 529.9 eV.[35] The C 1s spectrum shows a broad peak at 284 eV, stemming from the inhomogeneous perturbation of the C−Ir interaction induced in graphene regions covered by different amounts of intercalated oxygen. In the Ir $4f_{7/2}$ spectrum, the Ir1 component at 60.57 eV due to Ir atoms bound to one oxygen atom[35] increases at the expense of the S component.

An efficient intercalation starts for a substrate temperature of 500 K, while the complete intercalation is achieved at 520 K. This final step leads to a high-intensity O 1s peak, centered at 529.8 eV, and to a narrow C 1s spectrum peaked at 283.60 eV, which is 0.54 eV below the initial binding energy position. Now the graphene layer is "lifted" from the Ir surface; that is, it is decoupled from the Ir(111) through the adsorbed oxygen layer. The same intensity of the C 1s spectrum measured on the as-grown and on the O-intercalated graphene excludes that C atoms are etched during the exposure to O_2. The Ir $4f_{7/2}$ line shape has completely lost the S component and exhibits a new Ir2 feature at 61.08 eV, due to Ir atoms bound to two oxygen atoms.[35] We find a striking similarity between Ir $4f_{7/2}$ and O 1s spectra taken after intercalation and those measured on O/Ir(111), *i.e.*, in the absence of graphene (see bottom panels in Figure 1b and c). This indicates that O atoms adsorb predominantly in the 3-fold fcc hollow sites below graphene, as on the clean metal.[36]

The amount of oxygen intercalated below graphene at increasing temperature can be estimated by quantitatively comparing the Ir $4f_{7/2}$ and O 1s spectra with those measured during oxygen uptake on the clean Ir(111) surface at room temperature, which leads to a saturation coverage of $\theta = 0.38$ monolayers (ML)[35] (see Figure 1b, c). For an intercalation temperature of 520 K, we find an oxygen coverage of $\theta \approx 0.6$ ML. The higher oxygen coverage under graphene can be readily read from the Ir2/Ir1 ratio being higher than 1, the value expected for the O-(2×1) structure with 0.5 ML coverage. This estimation is based on the finding that, as pointed out above, also in the presence of graphene the O atoms adsorb in the fcc sites. This large coverage may be due to the higher oxygen pressure[36] used in the present work as compared to 1×10^{-7} mbar of ref 35 and to the presence of graphene locking the O atoms close to the metal surface.

The relation between the C 1s BE shift and the amount of intercalated oxygen is shown in Figure 1d. All data points were obtained by exposing to O_2 newly deposited graphene layers at temperatures ranging between 500 and 520 K and for 5 to 10 min exposure time. The curve shows that most of the C 1s binding energy shift is induced in the first part of the

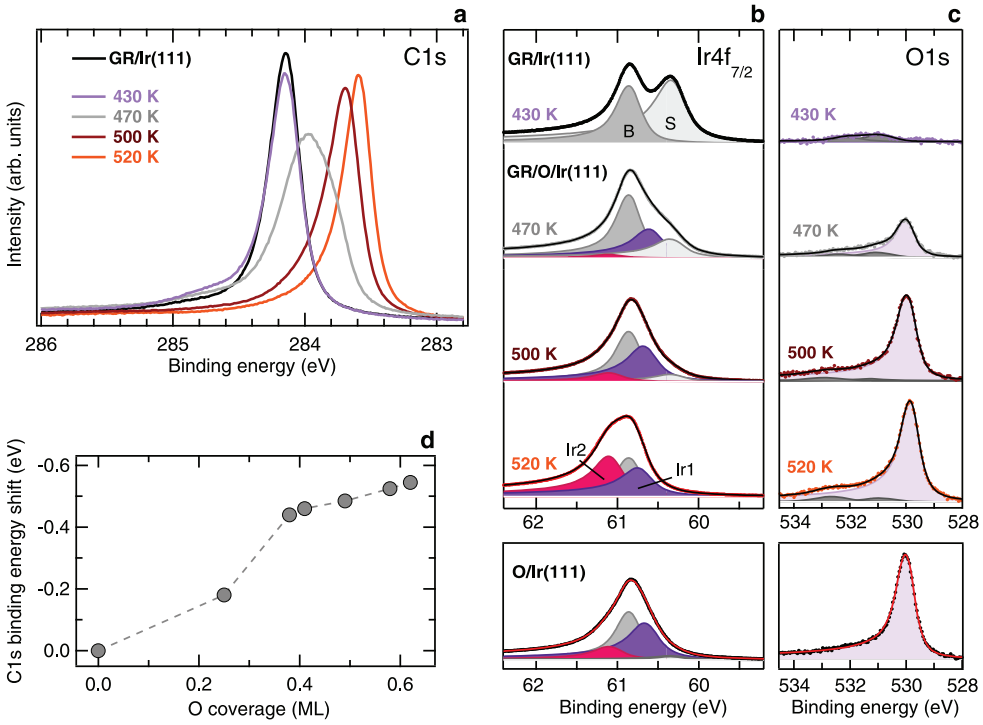

Figure 1. (a) C 1s, (b) Ir $4f_{7/2}$, and (c) O 1s core level spectra for different intercalation steps of oxygen under graphene/Ir(111). Oxygen was dosed through a doser at a pressure of 5×10^{-3} mbar for 10 min and at a sample temperature ranging from 430 to 520 K. The bottom panels in (b) and (c) show the Ir $4f_{7/2}$ and the O 1s spectra of the Ir(111) surface saturated with oxygen, with a coverage of θ = 0.38 ML. (d) Binding energy shift of the C 1s peak maximum as a function of the oxygen coverage.

intercalation: a coverage of ~0.4 ML induces a C 1s shift of −0.44 eV, whereas the subsequent increase to ~0.6 ML determines only an additional shift of −0.1 eV. This C 1s binding energy shift is attributed to the charge transfer from graphene to the electronegative oxygen, leading to hole-doped graphene.

The mechanism driving the intercalation of oxygen below graphene can be identified in the penetration of O_2 molecules through point defects and domain boundaries pre-existing in the graphene layer before the exposure to oxygen.[37] Similar routes have been identified in the case of Si[38] and ferromagnetic metal[25] atoms intercalating below entire graphene layers. We cannot exclude that during the exposure to oxygen new lattice vacancies with respect to as-grown graphene nucleate. This is likely to take place in the vicinity of defects or in correspondence with the wrinkles[32] that form in graphene/Ir(111) during cooling after the CVD growth.[13] However, the possible C loss during oxygen intercalation for a complete graphene layer at 520 K is below the XPS detection limit (1−2%).

The thermal stability of the O-intercalated graphene/Ir(111) interface, and the eventual deintercalation of oxygen, is explored by following the C 1s core level spectrum during sample annealing. Figure 2a shows the intensity plot derived from the sequence of spectra measured while ramping the sample temperature from 320 to 690 K with a rate of 0.5 K/s. The top and bottom spectra represent the high-resolution XPS C 1s spectra measured before and after annealing, respectively. The C 1s intensity plot indicates that the peak is quite stable up to 570 K and suddenly undergoes a rapid transition recovering the BE position and the line shape characteristic of the graphene/Ir(111) surface. The Ir $4f_{7/2}$ and O 1s spectra measured on the deintercalated surface are shown in Figure 2b and c, respectively. The Ir $4f_{7/2}$ spectrum exhibits the spectral line shape typical for the graphene/Ir(111) surface (see Figure 1b), whereas only negligible traces remain in the O 1s spectrum.

Thus after heating below 700 K and the consequent oxygen loss, the graphene layer has recovered its initial interaction with the Ir surface: it is "landed". The C 1s intensity, however, is ~18% lower than that of the as-grown graphene, implying that such an amount of C atoms has been lost in the deintercalation process.

The BE position of the C 1s peak measured during thermal annealing is taken as a probe of the oxygen deintercalation. The BE shift in Figure 2d, obtained from the series of spectra in Figure 2a, shows that up to $T \approx$ 570 K the C 1s upshifts by ~70 meV with a rate slightly increasing with temperature. According to the curve in Figure 1d, this shift can be related to a decrease of the O coverage from ~0.6 to ~0.45 ML. Then at around 600 K and within ~50 K the C 1s peak rapidly reaches the BE position typical for graphene/Ir(111), as indicated by the derivative d(BE)/dT, revealing that a sudden oxygen deintercalation has taken place.

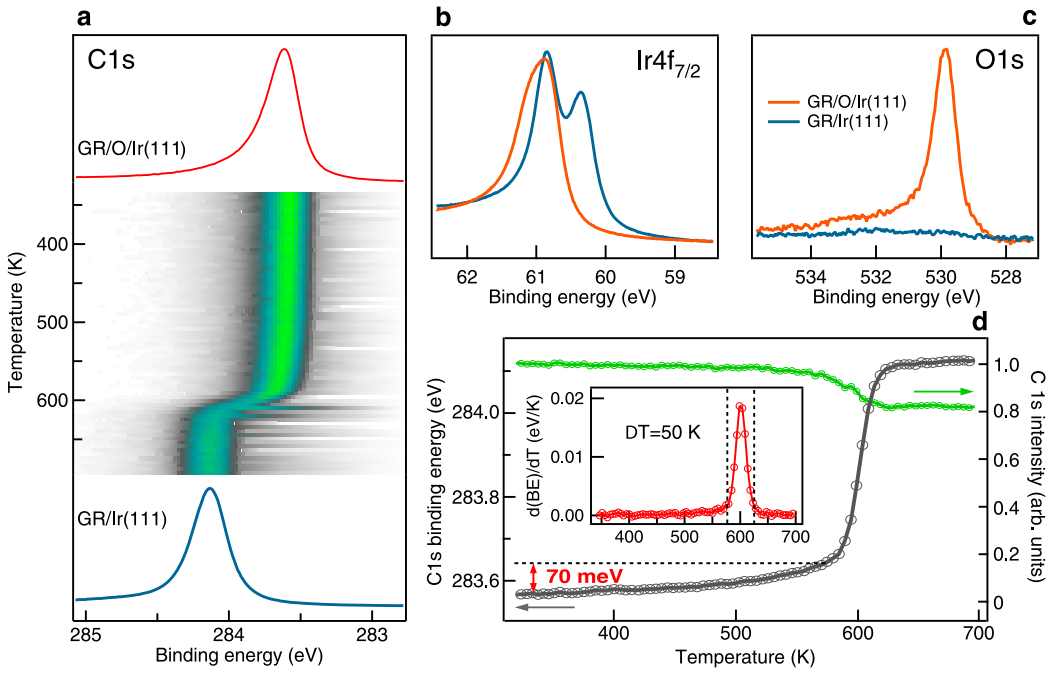

Figure 2. (a) C 1s thermal evolution measured on graphene/O/Ir(111) while ramping the temperature from 320 to 690 K at a rate of 0.5 K/s. The top and bottom spectra were measured before and after the annealing, respectively, while the central panel represents the C 1s intensity plot during sample heating. (b) Ir $4f_{7/2}$ and (c) O 1s spectra measured before and after oxygen deintercalation. (d) C 1s intensity and BE shift *vs* temperature as determined from the spectra in (a). The inset shows the first derivative of the BE.

In order to determine the mechanism driving the deintercalation, it must be kept in mind that desorption of the chemisorbed oxygen from the Ir(111) surface occurs only above 800 K.[39,40] This means that the oxygen loss observed below 650 K in this case cannot be due to the recombination of adsorbed oxygen leading to O_2 desorption from the metal surface. The slow oxygen loss observed up to 570 K may be due to the diffusion of the chemisorbed oxygen into the substrate, in agreement with early XPS studies reporting a decrease of the oxygen chemisorbed on Ir(111) for temperatures above 300 K due to subsurface diffusion.[41,42] In the present case, however, the simultaneous decrease of the C 1s intensity by a few percent might also suggest that the first 0.15 ML of oxygen is partly removed through low-rate etching events. When the oxygen coverage reaches ~0.45 ML, it is no longer sufficient to keep the graphene layer decoupled from the Ir surface. Therefore, the interaction between Ir and graphene is locally restored in the presence of the residual chemisorbed oxygen. At ~600 K, this results in the fast etching of the graphene layer. The products of this reaction, CO[32] or possibly CO_2, are not detected by XPS because of their short lifetime on Ir(111) at 600 K.[43,44] However, with only ~0.45 ML of oxygen available for the fast etching, the formation of CO would merely consume ~18% of the initial C amount of ~2.5 ML. An even smaller amount would be lost in the case of parallel reactions producing CO_2. The agreement with the 18% decrease in the C 1s intensity upon O deintercalation (green curve in Figure 2d) points toward the predominant formation of CO.

The abruptness of the fast oxygen deintercalation can be rationalized only by assuming that the chemisorbed oxygen undergoes a fast reaction from the whole surface, as any process involving the consumption of oxygen through oxidation of graphene edges would proceed at a much slower rate.[32,45] Similar abrupt deintercalation processes have been observed for incomplete monolayer graphene on Ru(0001).[32,31] It should be mentioned that oxygen has been suggested to deintercalate from graphene/O/Ru(0001) as O_2 at temperatures below the oxygen desorption threshold for the O/Ru(0001) system, due to the graphene-induced weakening of the O−Ru bonding strength.[31] In our case the balance between the amount of intercalated O and the quantity of C loss suggests that the main reaction leading to deintercalation is graphene oxidation to CO. However, the possibility that O_2 desorption is also taking place, due to the modified chemistry under the graphene cover, could be definitely ruled out only by performing programmed thermal desorption experiments.

The intercalation of oxygen under graphene on Ir(111) has a dramatic effect on the valence band electronic structure because the already small interaction between the metal and the graphene is weakened further. We follow this by angle-resolved photoemission (ARPES) measurements, which give direct access

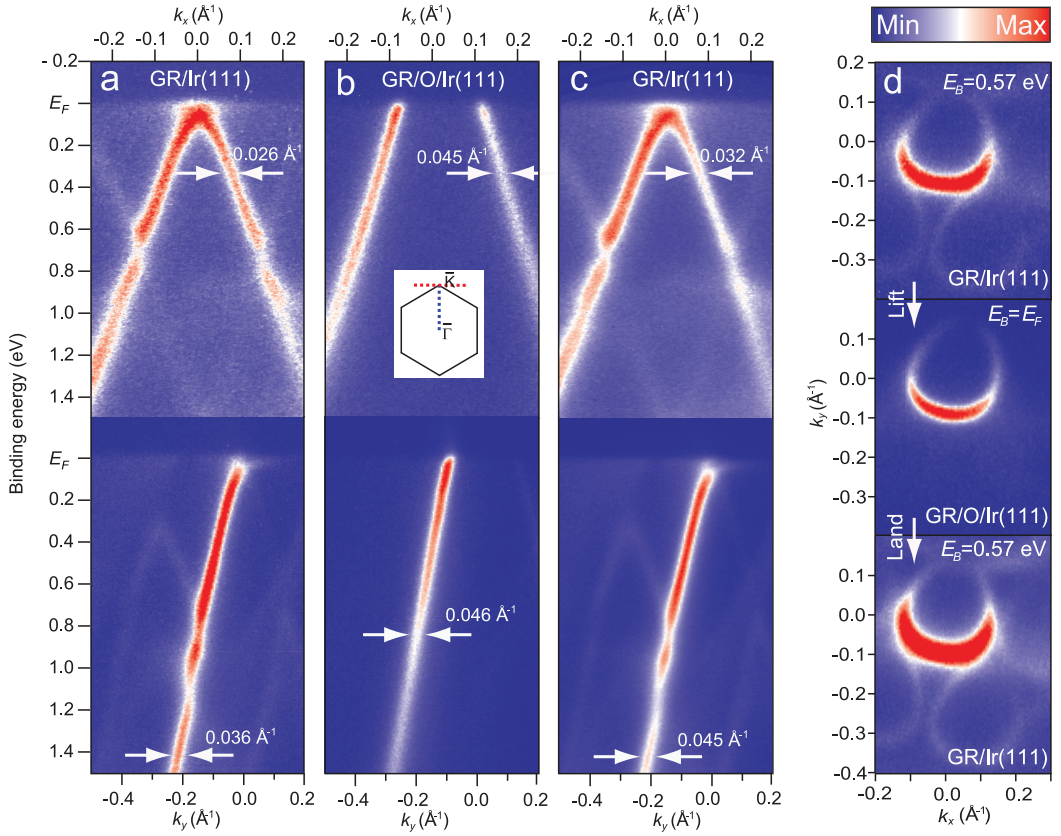

Figure 3. ARPES measurements of the spectral function of lifted and landed graphene on Ir(111). The spectra were acquired along a line orthogonal to the $\bar{\Gamma}\bar{K}$ direction ((a−c) top panels) and along the $\bar{\Gamma}\bar{K}$ direction ((a−c) bottom panels) in the Brillouin zone (see inset in (b)). The wavevector components $k_{||} = (k_x, k_y)$ are measured relative to the $\bar{K}$-point. (a) Dispersion of as-grown graphene/Ir(111), (b) lifted graphene due to O-intercalation, and (c) landed graphene following O-deintercalation. (d) Constant binding energy cuts at −0.64 eV from the Dirac point for clean, lifted, and landed graphene.

to the spectral function (or electronic band structure) of the system. The electronic structure changes upon lifting and landing graphene on Ir(111) are shown in Figure 3. For the pristine graphene on the Ir(111) system, we observe the narrow linearly dispersing π-band, forming the Dirac cone. The cone shows minigaps and weak replicas that are caused by the interaction with the substrate and the periodicity given by the moiré. The typical momentum distribution curve (MDC) line width determined 0.38 eV below the Fermi level is 0.026 Å^{-1}. The crossing point of the two π-band branches measured orthogonal to the $\bar{\Gamma}\bar{K}$ direction defines the Dirac point E_D, which is found at the binding energy $E_D = -0.067$ eV by linear extrapolation (see Methods). This reveals that the as-grown graphene is only slightly p-doped. All these findings are consistent with previous studies of the same system.[18,19]

A huge difference in the dispersion is observed in Figure 3b following oxygen intercalation. The band structure is similar to that of hydrogen-intercalated quasi free-standing graphene on SiC,[28,46] *i.e.*, without any signs of minigaps or replica bands.[47] The Dirac point is now far above the Fermi level at a binding energy of −0.64 eV, corresponding to a shift of 0.57 eV to lower binding energies compared to E_D of the as-grown graphene. This shift is interpreted as a doping effect caused by an electron transfer to the interfacial oxygen, and its magnitude is almost equal to the observed shift in the C 1s spectrum upon oxygen intercalation (see Figure 1d). The Fermi surface of the lifted graphene (Figure 3d central panel) shows a single Dirac cone without the replicas observed in the corresponding constant binding energy surface for the as-grown graphene (Figure 3d top panel). The clear asymmetry of the intensity distribution is a matrix element effect stemming from two-point interference effects from the two graphene sublattices.[48]

The MDC line width of the Dirac cone for lifted graphene measured orthogonal to the $\bar{\Gamma}\bar{K}$ direction (0.045 Å^{-1}) is wider than for the nonintercalated graphene (0.026 Å^{-1}) and for hydrogen-intercalated graphene on SiC (≈0.02 Å^{-1})[46] within a similar range of binding energies. Such differences can partly be related to the large p-doping, which shifts the dispersion considered here to lower binding energies, such that the analysis is carried out on a deeper part of the π-band where the phase space for scattering is larger. Another interpretation of a larger line width would be a poorer structural quality of the graphene on Ir as

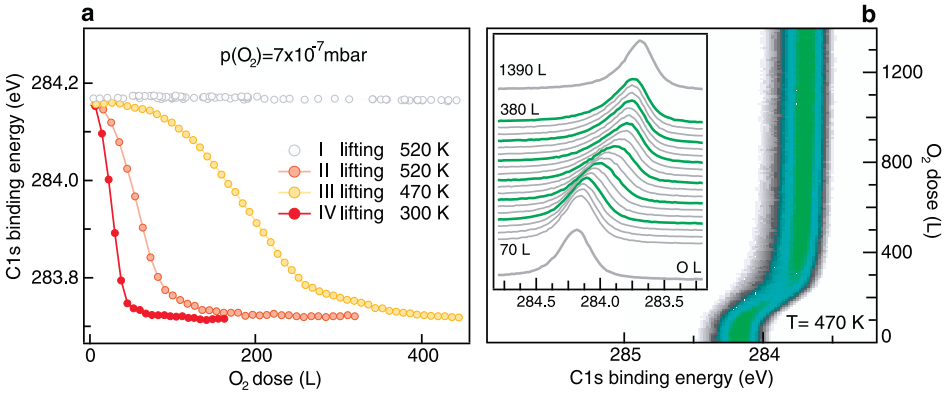

Figure 4. (a) C 1s binding energy measured during oxygen exposure at 7 × 10^{-7} mbar and different sample temperatures on the as-grown graphene/Ir(111) (I lifting) and for graphene/Ir(111) defected through previous intercalation/deintercalation cycles (II, III, and IV lifting); (b) C 1s intensity plot measured during the III lifting of defective graphene at T = 470 K. The inset shows the line shape evolution of the C 1s spectra.

opposed to SiC, giving rise to a shorter photohole lifetime. However, the width difference between the oxygen-lifted graphene on Ir(111) and the H-intercalated system on SiC could also be related to the different role of imperfectly doped areas in the two cases: on SiC, areas without H-intercalation would show the electronic structure of just the interface graphene layer on SiC. This interface layer does not show a Dirac cone,[9] and these areas would thus not contribute to the observed π-band or its line width. For lifted graphene on Ir(111), on the other hand, a nonuniform intercalation would still give rise to a Dirac cone from all areas, but the corresponding Dirac cones would be at slightly different binding energies, and this could give rise to a larger broadening. In this picture, the difference in line width between the two systems would thus be related to the different role of local doping variations and not to structural imperfections.

After oxygen deintercalation, the minigaps and replica bands are re-established along with the slight p-doping of the Dirac point (see Figure 3c and d bottom panel). Thus, the oxygen is removed from the metal interface, and the graphene is landed on the Ir surface, consistently with the XPS results in Figure 2. The process of oxygen removal does not cause any significant changes in the electronic structure of the landed graphene, even if, according to the intensity decrease in the C 1s spectrum in Figure 2d, ~18% of carbon is lost from the graphene lattice. We merely observe a small increase of the MDC line width compared to the initial preparation. This reflects the increased number of defects with the consequent reduction of the photohole lifetime.

Subsequent lifting and landing of the graphene by additional O intercalation/deintercalation cycles induce a more severe lattice damage, as the C vacancies formed after each deintercalation expose more defect sites readily available and highly reactive for further etching. Moreover the loss of 18% of C atoms in the first intercalation/deintercalation cycle is compatible with the presence of bare Ir regions, where O_2 molecules can dissociate and diffuse below graphene through edges and cracked defect lines, similarly to the modality proposed in refs 30 and 31 for incomplete graphene. The combination of these processes decreases the chemical potential to decouple graphene from the substrate, as illustrated in Figure 4a. The curves report the BE positions of the C 1s peak measured during the exposure to O_2 at a pressure of 7 × 10^{-7} mbar.

The flat curve measured at T = 520 K shows that the as-grown graphene does not allow for any oxygen intercalation. However, after a first intercalation at higher O_2 pressure followed by deinteraclation, the second lifting performed at T = 520 K occurs very rapidly owing to the reduced C coverage that facilitates the access of oxygen below graphene.

The effect of the temperature is evident in the third lifting performed at T = 470 K. Even if graphene is more defective than in the second lifting, a lower intercalation rate is observed, most probably due to the reduced mobility of the O atoms on Ir(111) at this temperature. The C 1s intensity plot and some selected C 1s spectra acquired during the third lifting are shown in Figure 4b: a marked change of the C 1s line shape is observed, while the stable C 1s spectral intensity during the whole oxygen exposure excludes that the interaction with O_2 molecules etches the already defected graphene lattice. This behavior is similar to that observed during the lifting at high O_2 pressure of the as-grown graphene (Figure 1).

The C loss in the first, second, and third landing was estimated to be around 18%, 23%, and 27% of the initial coverage of each cycle, respectively. This means that at the fourth lifting the initial C coverage of ~2.5 ML is reduced by more than 50%. Consistently, the red curve in Figure 4a shows that this strongly defective graphene can be lifted even at room temperature. It is worth noting that the curves in Figure 4a show a total BE shift ranging from −0.44 to −0.47 eV, which is lower

than that observed after the first lifting of Figure 1 (−0.54 eV), in agreement with the lower O coverage on the Ir(111) surface reached by dosing oxygen at a pressure in the 10^{-7} mbar range.

CONCLUSIONS

We demonstrate that it is possible to decouple an entire monolayer of epitaxial graphene from its Ir(111) substrate by oxygen intercalation. The completeness of the graphene layer was stated by XPS with an uncertainty of 1−2%. By properly selecting temperature and O_2 pressure we found the conditions to lift the full layer while keeping the etching rate low enough that possible C loss during intercalation is below 1−2%. The lack of bare Ir regions where O_2 could dissociate implies that molecular oxygen penetrates through graphene defects and dissociates on the metal surface below graphene. The process produces heavily p-doped, quasi free-standing graphene with a linear π-band dispersion unmodified by the substrate. Abrupt oxygen deintercalation with a slight carbon etching occurs around 600 K. The graphene is thus landed on the Ir(111) surface and recovers the substrate interaction, as witnessed by the reappearance of minigaps and replica bands in the spectral function. The graphene etching induced by the first deintercalation renders the subsequent oxygen intercalation much easier, as oxygen intercalation cycles proceed readily at lower pressure and temperature. Repeated intercalation/deintercalation cycles cause further damage of the graphene up to a level that it can be lifted from the Ir(111) surface at room temperature and moderate O_2 pressure. The results are expected to provide new means for fundamental studies on graphene, where free-standing, highly ordered, and extended layers of graphene are of utmost importance. Moreover, thanks to the stability of the intercalated system in a wide temperature range, they could pave the way for the advancement of next-generation graphene-based electronics exploiting the properties of stand-alone graphene.

METHODS

A graphene monolayer was grown by doing more than 10 cycles of temperature-programmed growth, consisting in dosing ethylene at 520 K then annealing to 1470 K, followed by a prolonged annealing at high temperature with a base ethylene pressure of 1×10^{-7} mbar. This ensures the growth of a complete layer of graphene that does not leave bare Ir regions.[18,19] The completeness of the graphene layer was proved by the ratio between the intensities of the C 1s and Ir 4f spectra taken at normal emission at a photon energy of 400 eV, which reached a saturation and did not change by prolonging the growth time. This method detects variations of the C coverage as low as 1−2%.

The sample quality was checked both with low-energy electron diffraction, providing an intense moiré pattern for a clean graphene monolayer, and with photoemission from the C 1s and the Ir $4f_{7/2}$ core levels and the graphene π-band. Intercalation of oxygen was achieved by placing the sample in front of a custom-made O_2 doser and maintaining the background O_2 pressure at 5×10^{-4} mbar. With this setup we estimate that the pressure at the sample surface is $\sim 5 \times 10^{-3}$ mbar. For defective graphene, oxygen intercalation was achieved by exposing the sample to a background O_2 pressure of 7×10^{-7} mbar.

The high-energy-resolution XPS experiments were performed at the SuperESCA beamline of the synchrotron radiation source Elettra (Trieste, Italy). Ir $4f_{7/2}$, C 1s, and O 1s core level spectra were measured at a photon energy of 130, 400, and 650 eV, respectively, with an overall energy resolution ranging from 40 to 150 meV. For each spectrum, the binding energy was calibrated by measuring the Fermi level position of the Ir substrate. The measurements were performed with the photon beam impinging at grazing incidence (70°), while photoelectrons were collected at normal emission angle. The core level spectra were best fitted with Doniach−Šunjić functions convoluted with Gaussians, and a linear background.

The ARPES measurements were carried out at the SGM-3 beamline of the synchrotron radiation source ASTRID (Aarhus, Denmark) with the sample temperature kept at 70 K. The photon energy was 47 eV, and the total energy and k resolution amounted to 18 meV and 0.01 $Å^{-1}$, respectively. To estimate the Dirac point binding energy from the measured spectral function, the peak positions of MDCs corresponding to the left and right branches of the π-band are extracted over a range of binding energies from 0.3 to 0.6 eV below the Fermi level and linearly extrapolated. This range was chosen to improve experimental uncertainties and avoid well-known fitting errors due to the minigaps and the electron−phonon coupling-induced kinks in the dispersion.[49]

Conflict of Interest: The authors declare no competing financial interest.

Acknowledgment. This work was supported by The Danish Council for Independent Research/Technology and Production Sciences and the Lundbeck Foundation. A.B. acknowledges the Universitá degli Studi di Trieste for the Finanziamento per Ricercatori di Ateneo. R.L. thanks the support of the COST Action MP0901 "NanoTP".

REFERENCES AND NOTES

1. N'Diaye, A. T.; Coraux, J.; Plasa, T. P.; Busse, C.; Michely, T. Structure of Epitaxial Graphene on Ir(111). *New J. Phys.* **2008**, *10*, 043033.
2. Coraux, J.; N'Diaye, A. T.; Busse, C.; Michely, T. Structural Coherency of Graphene on Ir(111). *Nano Lett.* **2008**, *8*, 565–570.
3. N'Diaye, A. T.; Bleikamp, S.; Feibelman, P. J.; Michely, T. Two-Dimensional Ir Cluster Lattice on a Graphene Moiré on Ir(111). *Phys. Rev. Lett.* **2006**, *97*, 215501.
4. Sutter, P. W.; Flege, J.-I.; Sutter, E. A. Epitaxial Graphene on Ruthenium. *Nat. Mater.* **2008**, *7*, 406–411.
5. Dedkov, Y. S.; Fonin, M.; Rudiger, U.; Laubschat, C. Rashba Effect in the Graphene/Ni(111) System. *Phys. Rev. Lett.* **2008**, *100*, 107602.
6. Sutter, P.; Sadowski, J. T.; Sutter, E. Graphene on Pt(111): Growth and Substrate Interaction. *Phys. Rev. B* **2009**, *80*, 245411.
7. Sicot, M.; Bouvron, S.; Zander, O.; Rüdiger, U.; Dedkov, Y. S.; Fonin, M. Nucleation and Growth of Nickel Nanoclusters on Graphene Moiré on Rh(111). *Appl. Phys. Lett.* **2010**, *96*, 093115.
8. Bostwick, A.; Ohta, T.; Seyller, T.; Horn, K.; Rotenberg, E. Quasiparticle Dynamics in Gaphene. *Nat. Phys.* **2007**, *3*, 36–40.
9. Emtsev, K. V.; Speck, F.; Seyller, T.; Ley, L.; Riley, J. D. Interaction, Growth, and Ordering of Epitaxial Graphene on SiC(0001) Surfaces: A Comparative Photoelectron Spectroscopy Study. *Phys. Rev. B* **2008**, *77*, 155303.

10. Huang, H.; Chen, W.; Chen, S.; Wee, A. T. S. Bottom-up Growth of Epitaxial Graphene on 6H-SiC(0001). *ACS Nano* **2008**, *2*, 2513–2518.
11. Robinson, J.; Weng, X.; Trumbull, K.; Cavalero, R.; Wetherington, M.; Frantz, E.; LaBella, M.; Hughes, Z.; Fanton, M.; Snyder, D. Nucleation of Epitaxial Graphene on SiC(0001). *ACS Nano* **2009**, *4*, 153–158.
12. Novoselov, K. S.; Geim, A. K.; Morozov, S. V.; Jiang, D.; Zhang, Y.; Dubonos, S. V.; Grigorieva, I. V.; Firsov, A. A. Electric Field Effect in Atomically Thin Carbon Films. *Science* **2004**, *306*, 666–669.
13. Hattab, H.; N'Diaye, A. T.; Wall, D.; Klein, C.; Jnawali, G.; Coraux, J.; Busse, C.; van Gastel, R.; Poelsema, B.; Michely, T.; *et al*. Interplay of Wrinkles, Strain, and Lattice Parameter in Graphene on Iridium. *Nano Lett.* **2012**, *12*, 678–682.
14. Morozov, S. V.; Novoselov, K. S.; Katsnelson, M. I.; Schedin, F.; Elias, D. C.; Jaszczak, J. A.; Geim, A. K. Giant Intrinsic Carrier Mobilities in Graphene and Its Bilayer. *Phys. Rev. Lett.* **2008**, *100*, 016602.
15. Chen, J.-H.; Jang, C.; Xiao, S.; Ishigami, M.; Fuhrer, M. S. Intrinsic and Extrinsic Performance Limits of Graphene Devices on SiO_2. *Nat. Nanotechnol.* **2008**, *3*, 206–209.
16. Wang, B.; Caffio, M.; Bromley, C.; Früchtl, H.; Schaub, R. Coupling Epitaxy, Chemical Bonding, and Work Function at the Local Scale in Transition Metal-Supported Graphene. *ACS Nano* **2010**, *4*, 5773–5782.
17. Miniussi, E.; Pozzo, M.; Baraldi, A.; Vesselli, E.; Zhan, R. R.; Comelli, G.; Mentes, T. O.; Niño, M. A.; Locatelli, A.; Lizzit, S.; *et al*. Thermal Stability of Corrugated Epitaxial Graphene Grown on Re(0001). *Phys. Rev. Lett.* **2011**, *106*, 216101.
18. Pletikosic, I.; Kralj, M.; Pervan, P.; Brako, R.; Coraux, J.; N'Diaye, A. T.; Busse, C.; Michely, T. Dirac Cones and Minigaps for Graphene on Ir(111). *Phys. Rev. Lett.* **2009**, *102*, 056808.
19. Kralj, M.; Pletikosić, I.; Petrović, M.; Pervan, P.; Milun, M.; N'Diaye, A. T.; Busse, C.; Michely, T.; Fujii, J.; Vobornik, I. Graphene on Ir(111) Characterized by Angle-Resolved Photoemission. *Phys. Rev. B* **2011**, *84*, 075427.
20. Merino, P.; Švec, M.; Pinardi, A. L.; Otero, G.; Martn-Gago, J. Strain-Driven Moiré Superstructures of Epitaxial Graphene on Transition Metal Surfaces. *ACS Nano* **2011**, *5*, 5627–5634.
21. Varykhalov, A.; Sanchez-Barriga, J.; Shikin, A. M.; Biswas, C.; Vescovo, E.; Rybkin, A.; Marchenko, D.; Rader, O. Electronic and Magnetic Properties of Quasifreestanding Graphene on Ni. *Phys. Rev. Lett.* **2008**, *101*, 157601.
22. Huang, L.; Pan, Y.; Pan, L.; Gao, M.; Xu, W.; Que, Y. Z. H.; Wang, Y.; Du, S.; Gao, H.-J. Intercalation of Metal Islands and Films at the Interface of Epitaxially Grown Graphene and Ru(0001) Surfaces. *Appl. Phys. Lett.* **2011**, *99*, 163107.
23. Voloshina, E. N.; Generalov, A.; Weser, M.; Böttcher, S.; Horn, K.; Dedkov, Y. S. Structural and Electronic Properties of the Graphene/Al/Ni(111) Intercalation System. *New J. Phys.* **2011**, *13*, 113028.
24. Enderlein, C.; Kim, Y. S.; Bostwick, A.; Rotenberg, E.; Horn, K. The Formation of an Energy Gap in Graphene on Ruthenium by Controlling the Interface. *New J. Phys.* **2010**, *12*, 033014.
25. Sicot, M.; Leicht, P.; Zusan, A.; Bouvron, S.; Zander, O.; Weser, M.; Dedkov, Y. S.; Horn, K.; Fonin, M. Size-Selected Epitaxial Nanoislands Underneath Graphene Moiré on Rh(111). *ACS Nano* **2012**, *6*, 151–158.
26. Mao, J.; Huang, L.; Pan, Y.; Gao, M.; He, J.; Zhou, H.; Guo, H.; Tian, Y.; Zou, Q.; Zhang, L.; *et al*. Silicon Layer Intercalation of Centimeter-Scale, Epitaxially Grown Monolayer Graphene on Ru(0001). *Appl. Phys. Lett.* **2012**, *100*, 093101.
27. Wong, S. L.; Huang, H.; Wang, Y.; Cao, L.; Qi, D.; Santoso, I.; Chen, W.; Wee, A. T. S. Quasi-Free-Standing Epitaxial Graphene on SiC (0001) by Fluorine Intercalation from a Molecular Source. *ACS Nano* **2011**, *5*, 7662–7668.
28. Riedl, C.; Coletti, C.; Iwasaki, T.; Zakharov, A. A.; Starke, U. Quasi-Free-Standing Epitaxial Graphene on SiC Obtained by Hydrogen Intercalation. *Phys. Rev. Lett.* **2009**, *103*, 246804.
29. Bostwick, A.; Speck, F.; Seyller, T.; Horn, K.; Polini, M.; Asgari, R.; MacDonald, A. H.; Rotenberg, E. Observation of Plasmarons in Quasi-Freestanding Doped Graphene. *Science* **2010**, *328*, 999–1002.
30. Zhang, H.; Fu, Q.; Cui, Y.; Tan, D.; Bao, X. Growth Mechanism of Graphene on Ru(0001) and O_2 Adsorption on the Graphene/Ru(0001) Surface. *J. Phys. Chem. C* **2009**, *113*, 8296–8301.
31. Sutter, P.; Sadowski, J. T.; Sutter, E. A. Chemistry under Cover: Tuning Metal-Graphene Interaction by Reactive Intercalation. *J. Am. Chem. Soc.* **2010**, *132*, 8175–8179.
32. Starodub, E.; Bartelt, N. C.; McCarty, K. F. Oxidation of Graphene on Metals. *J. Phys. Chem. C* **2010**, *114*, 5134–5140.
33. Lacovig, P.; Pozzo, M.; Alfè, D.; Vilmercati, P.; Baraldi, A.; Lizzit, S. Growth of Dome-Shaped Carbon Nanoislands on Ir(111): The Intermediate between Carbidic Clusters and Quasi-Free-Standing Graphene. *Phys. Rev. Lett.* **2009**, *103*, 166101.
34. Larciprete, R.; Fabris, S.; Sun, T.; Lacovig, P.; Baraldi, A.; Lizzit, S. Dual Path Mechanism in the Thermal Reduction of Graphene Oxide. *J. Am. Chem. Soc.* **2011**, *133*, 17315–17321.
35. Bianchi, M.; Cassese, D.; Cavallin, A.; Comin, R.; Orlando, F.; Postregna, L.; Golfetto, E.; Lizzit, S.; Baraldi, A. Surface Core Level Shifts of Clean and Oxygen Covered Ir(111). *New J. Phys.* **2009**, *11*, 063002.
36. Zhang, H.; Soon, A.; Delley, B.; Stampfl, C. Stability, Structure, and Electronic Properties of Chemisorbed Oxygen and Thin Surface Oxides on Ir(111). *Phys. Rev. B* **2008**, *78*, 045436.
37. Banhart, F.; Kotakoski, J.; Krasheninnikov, A. V. Structural Defects in Graphene. *ACS Nano* **2011**, *5*, 26–41.
38. Xia, C.; Watcharinyanon, S.; Zakharov, A. A.; Yakimova, R.; Hultman, L.; Johansson, I.; Virojanadara, C. Si Intercalation/Deintercalation of Graphene on 6H-SiC(0001). *Phys. Rev. B* **2012**, *85*, 045418.
39. Hagen, D. J.; Nieuwenhhuys, B. E.; Rovida, G.; Somorjai, G. A. Low-Energy Electron Diffraction, Auger Electron Spectroscopy, and Thermal Desorption Studies of Chemisorbed CO and O_2 on the (111) and Stepped [6(111)×(100)] Iridium Surfaces. *Surf. Sci.* **1976**, *57*, 632–650.
40. Cornish, J. C. L.; Avery, N. R. Adsorption of N_2, O_2, N_2O and NO on Ir(111) by EELS and TPD. *Surf. Sci.* **1990**, *235*, 209–216.
41. Zhdan, P. A.; Boreskov, G. K.; Boronin, A.; Egelhoff, W. F.; Weinberg, W. H.; An, X. P. S. Investigation of the Chemisorption of Oxygen on the Iridium (111) Surface. *Surf. Sci.* **1976**, *61*, 25–36.
42. Marinova, Ts. S.; Kostov, K. L. Interaction of Oxygen with a Clean Ir(111) Surface. *Surf. Sci.* **1987**, *185*, 203–212.
43. Lauterbach, J.; Boyle, R. W.; Schick, M.; Mitchell, W. J.; Meng, B.; Weinberg, W. H. The Adsorption of CO on Ir(111) Investigated with FT-IRAS. *Surf. Sci.* **1996**, *350*, 32–44.
44. Wehner, S.; Baumann, F.; Ruckdeschel, M.; Kuppers, J. Kinetic Phase Transitions in the Reaction CO + O −> CO_2 on Ir(111) Surfaces. *J. Chem. Phys.* **2003**, *119*, 6823–6831.
45. Cui, Y.; Fu, Q.; Zhang, H.; Tan, D.; Bao, X. Dynamic Characterization of Graphene Growth and Etching by Oxygen on Ru(0001) by Photoemission Electron Microscopy. *J. Phys. Chem. C* **2009**, *113*, 20365–20370.
46. Forti, S.; Emtsev, K. V.; Coletti, C.; Zakharov, A. A.; Riedl, C.; Starke, U. Large-Area Homogeneous Quasifree Standing Epitaxial Graphene on SiC(0001): Electronic and Structural Characterization. *Phys. Rev. B* **2011**, *84*, 125449.
47. Pletikosic, I.; Kralj, M.; Milun, M.; Pervan, P. Finding the Bare Band: Electron Coupling to Two Phonon Modes in Potassium-Doped Graphene on Ir(111). *Phys. Rev. B* **2012**, *85*, 155447.
48. Shirley, E. L.; Terminello, L. J.; Santoni, A.; Himpsel, F. J. Brillouin-Zone-Selection Effects in Graphite Photoelectron Angular Distributions. *Phys. Rev. B* **1995**, *51*, 13614–13622.
49. Nechaev, I. A.; Jensen, M. F.; Rienks, E. D. L.; Silkin, V. M.; Echenique, P. M.; Chulkov, E. V.; Hofmann, P. Hole Dynamics in a Two-Dimensional Spin-Orbit Coupled Electron System: Theoretical and Experimental Study of the Au(111) Surface State. *Phys. Rev. B* **2009**, *80*, 113402.